

Rapid Flow Simulations

Computer simulations have helped to elucidate the rheology of rapid granular flows and allowed evaluation of some of the approximations inherent in the theoretical kinetic theory models. For example, the shape of the fluctuation velocity distributions begins to deviate from Maxwellian and the velocity fluctuations become more and more non-isotropic as the solids fraction approaches the maximum shearable value. These kinds of details require computer simulations and were explored, for example in the *hard particle* simulations of shear and chute flows by Campbell and Brennen (1985a,b). More generally, they represent the kinds of organized microstructure that can characterize granular flows close to the maximum shearable solids fraction. We briefly review some of the characteristics of granular flows revealed in the Campbell and Brennen simulations.

Among the first computer simulations were the two-dimensional flows of circular discs down an inclined plane (Campbell and Brennen 1985a). These utilize periodic longitudinal boundaries in which the particles re-enter the calculational space as depicted in Figure 1 and the simulation continues until a *quasi-steady* state is reached. Typical snapshots of the disc positions after a steady state has been reached are shown in

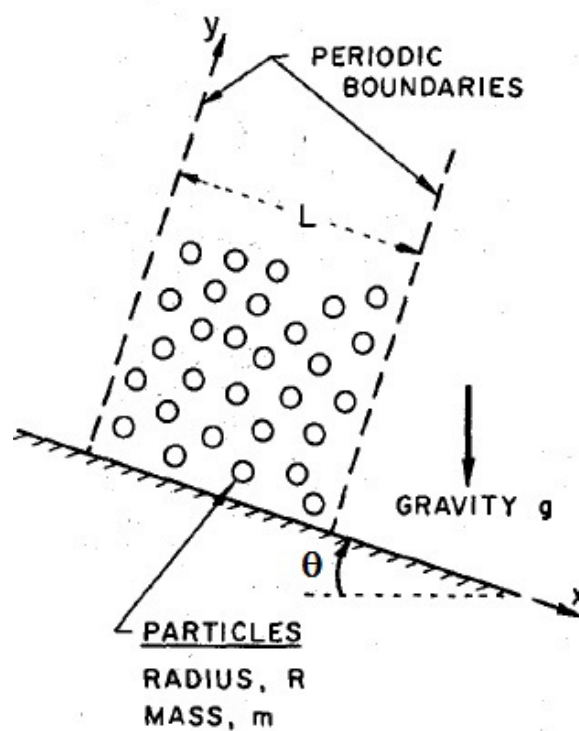


Figure 1: Computational domain for the two-dimensional flow of circular discs down an inclined plane of inclination, θ .

Figure 2 and display several of the significant features of these flows that are also exemplified by Figures 3 and 4. The $\theta = 30^\circ$ simulation is typical and the profiles of mean velocity, solid fraction and translational granular temperature for that case are shown in Figure 3. The translational granular temperature is simply a measure of the random velocities of the grains or discs. This is particularly high close to the wall due to the particle collisions with that boundary and those elevated random motions cause local rarefaction of the material in that region. This, in turn, leads to the reduced solid fraction in that region as is evident in

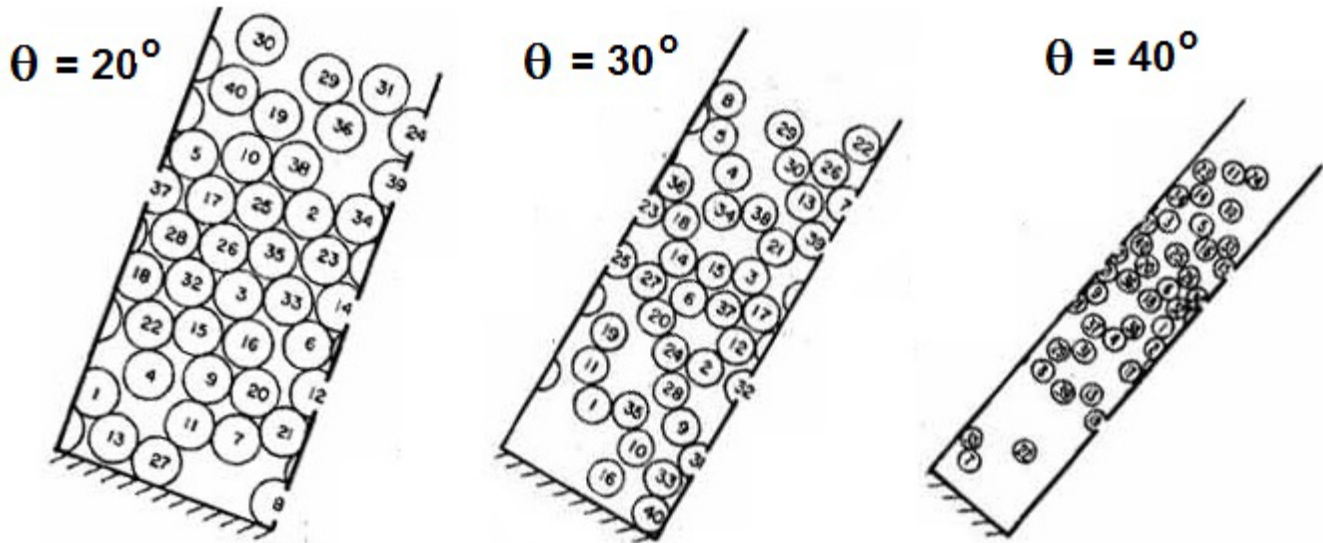


Figure 2: Snapshots from Campbell and Brennen (1985a) of three two-dimensional flows of circular discs down an inclined plane for three different inclinations, θ .

Figure 2 and is manifest in the middle graph of Figure 3. Furthermore the decrease in the magnitude of the random motions with distance from the wall creates a granular temperature gradient and therefore granular heat is conducted up into the layers further from the wall. Thus the simulations allowed evaluation of the

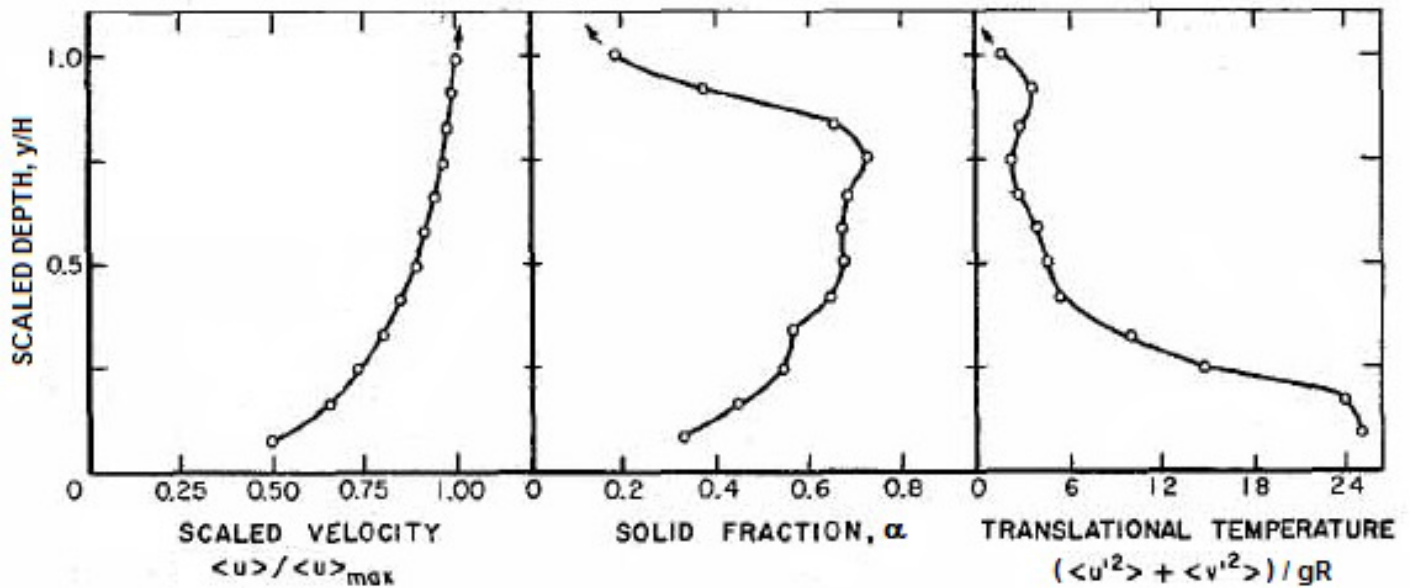


Figure 3: Profiles of the mean velocity, solid fraction and translational granular temperature for the $\theta = 30^\circ$ flows of Figure 2.

granular conductivity and its dependence on the solid fraction. The slower and denser $\theta = 20^\circ$ simulation also exhibits another general feature of granular flows. Because the granular temperatures in the middle layers of that flow fall below a critical level, the solid fraction becomes too high to allow shearing and the middle layers move as a solid, unshearing block as seen in Figure 4. Of course, the details of these chute flows do depend on the ratio of the layer depth to particle size and the coefficients governing the particle-particle and particle-wall collisions.

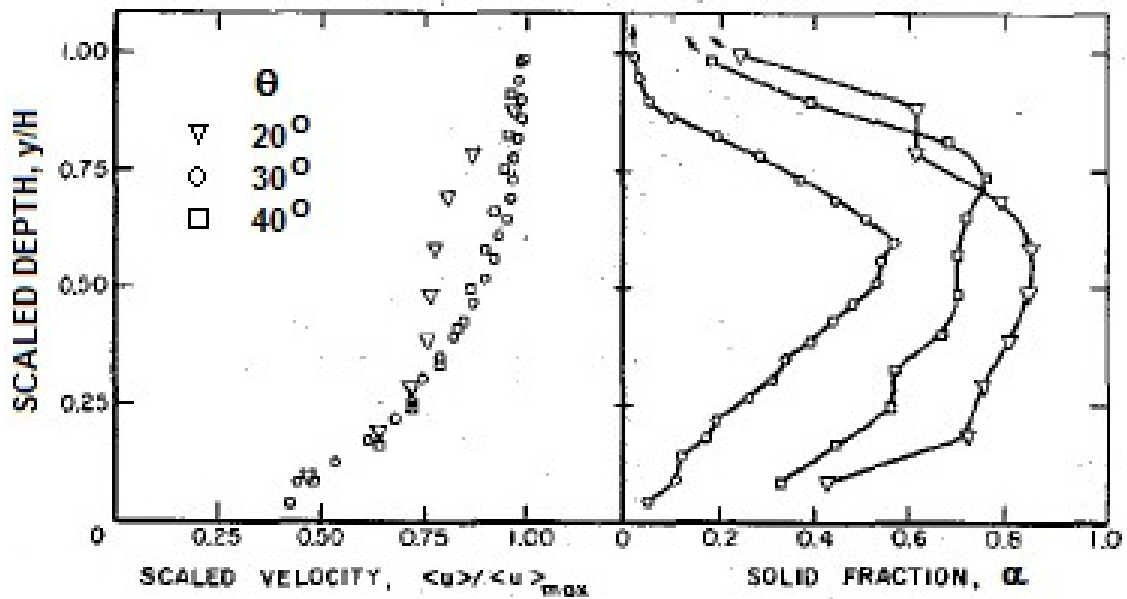


Figure 4: Profiles of the mean velocity and solid fraction in the flows of Figure 2.

Campbell and Brennen (1985b) used the same methodologies to simulate shear flows (Couette flows) between a static plate and a plate moving with velocity, U , in its own plane as depicted in Figure 5.

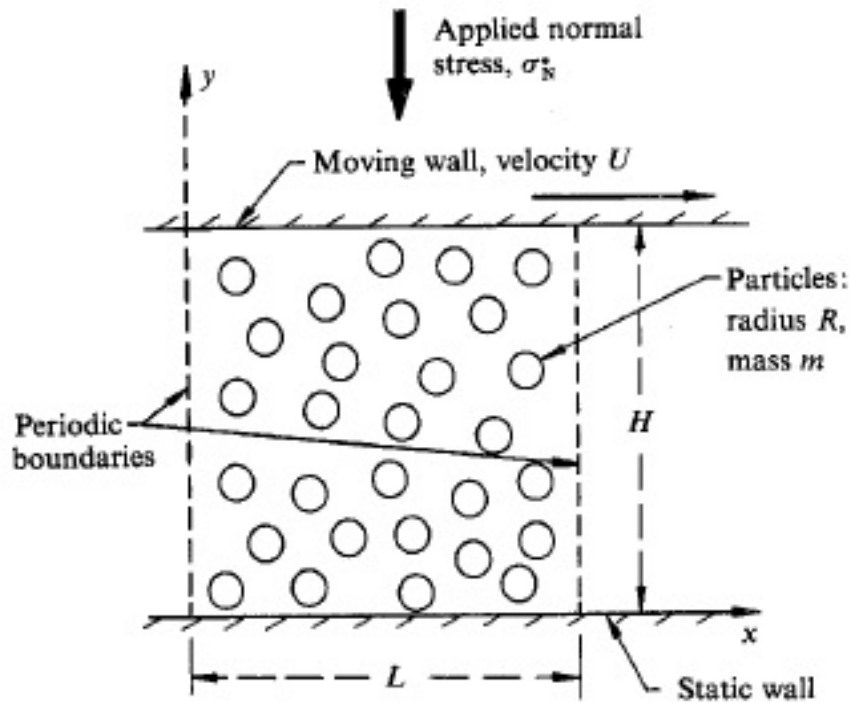


Figure 5: Computational domain for the two-dimensional flow of circular discs in a shear flow between two solid plates.

Figure 6 presents snapshots of three two-dimensional shear flows of circular discs with three different solids fractions, α . These calculations require a different strategy than with conventional fluids. The gap, H , is allowed to expand against a chosen spring stiffness so as to adjust to a stipulated normal stress, σ_N . This, in turn, allows the average solid fraction, α , to adjust to a value consistent with that normal stress. Figure

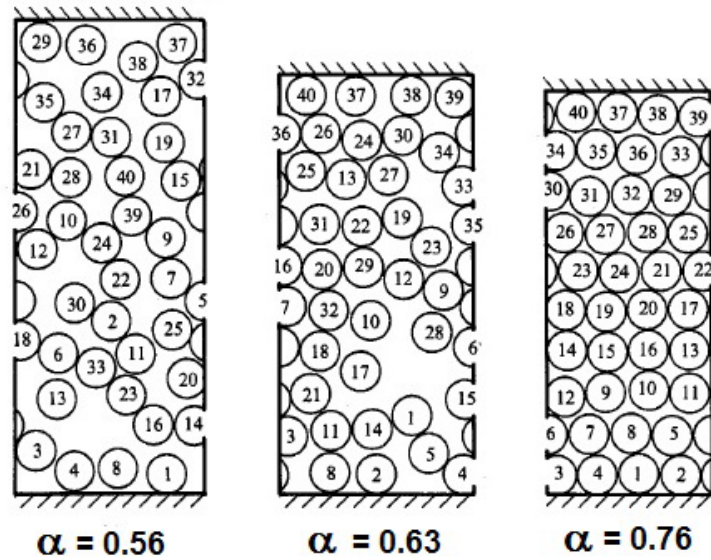


Figure 6: Snapshots from Campbell and Brennen (1985b) of three two-dimensional shear flows of circular discs with three different solids fractions, α .

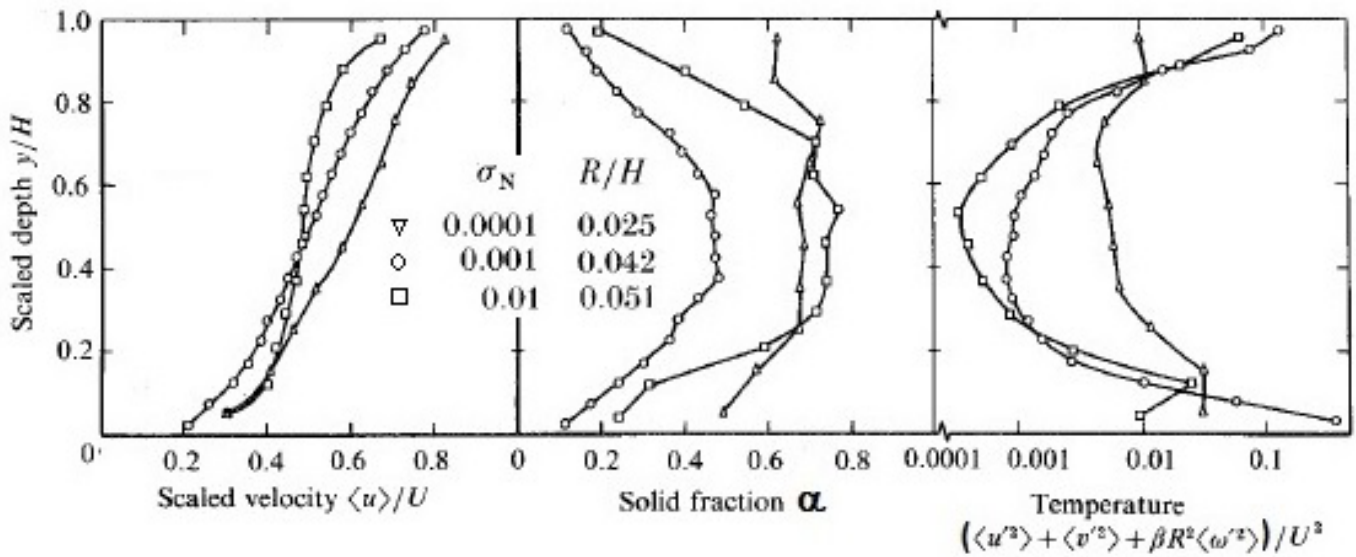


Figure 7: Profiles of the mean velocity, average solid fraction and granular temperature for the three simulations of Figure 6.

7 shows the velocity, average solid fraction and granular temperature for the same three flows shown in Figure 6; the stipulated normal stress and the resulting gap width, H , are shown in the included table. Note that at the highest normal stress ($\alpha = 0.72$) the core of the flow has almost reached a maximum unsharable state and this is reflected in the almost uniform velocity profile and the low core granular temperature. Figure 8 shows how the overall friction coefficient, σ_{xy}/σ_{yy} , varies with the average solid fraction for two different coefficients of restitution, ϵ . The results seem consistent with the experimental measurements of Savage and Sayed (1984) and with the two theoretical values of Jenkins and Savage (1983).

By further examining the statistics of the particle-particle collisions in these shear flow simulations Campbell and Brennen (1985b) found that developing microstructure could be readily detected and was manifest in the angular distribution of collision orientations within the shear flow. Typical collision angle probabil-

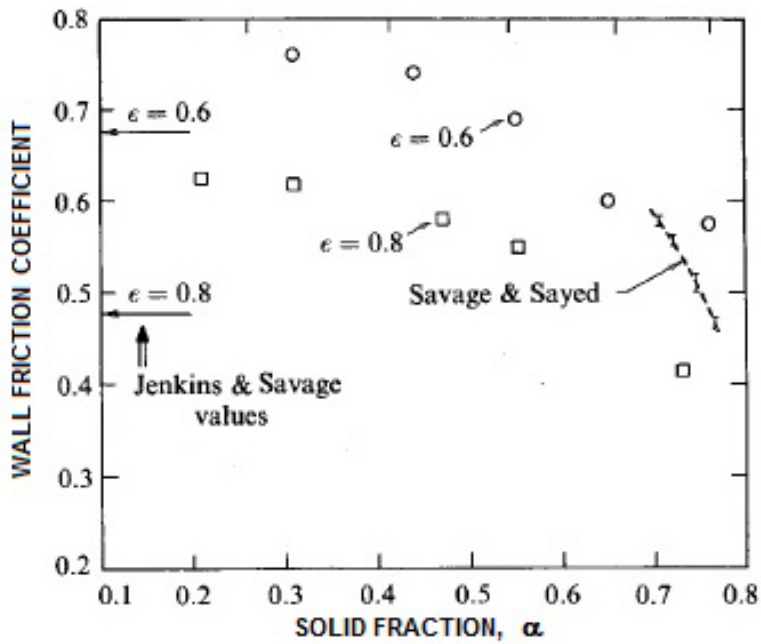


Figure 8: The wall friction coefficient as a function of the solid fraction, α , for the granular shear flows of Campbell and Brennen (1985b) with two different particle coefficients of restitution, $\epsilon = 0.6$ and 0.8 . Also shown are the experimental measurements of Savage and Sayed (1984) and two theoretical values from Jenkins and Savage (1983).

ity distributions for the shear flows of Figures 6 and 7 for various solid fractions, α , are shown in Figure 9. At the lower average solid fractions the dominant collision orientation involves collisions in the second and fourth quadrants. However, as the average solid fraction increases collision orientation peaks appear that result from sliding collisions between the packed layers. These changes in the statistics of the

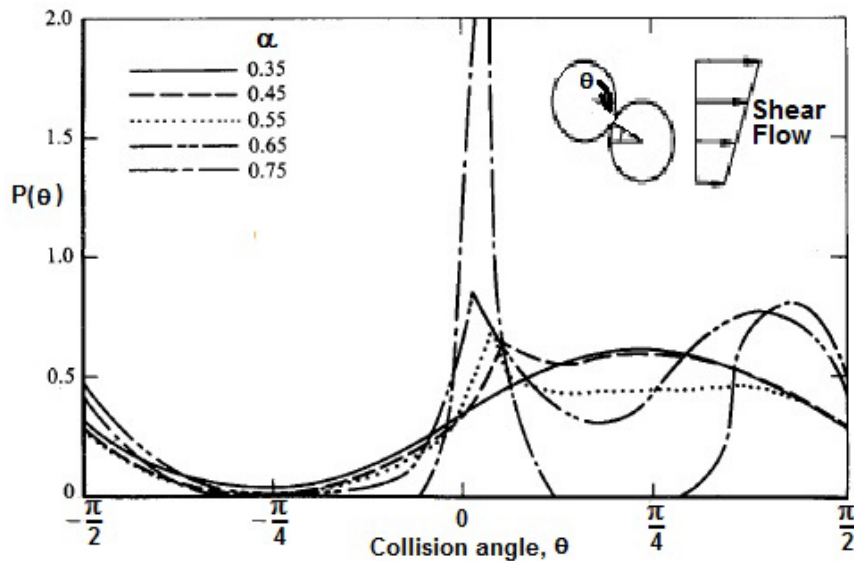


Figure 9: Typical collision angle probability distributions for the shear flows of Figures 6 and 7 for various solid fractions, α , taken from Campbell and Brennen (1985b).

microstructure must be incorporated in any theoretical model of the rheology of dense granular flows.